Continued increase of extreme El Niño frequency long after 1.5 °C warming stabilization

Article *in* Nature Climate Change · July 2017

DOI: 10.1038/nclimate3351

LETTERS
PUBLISHED ONLINE: 24 JULY 2017 | DOI: 10.1038/NCLIMATE3351

nature climate change

Continued increase of extreme El Niño frequency long after 1.5 °C warming stabilization

Guojian Wang[1,2], Wenju Cai[1,2*], Bolan Gan[1], Lixin Wu[1*], Agus Santoso[2,3], Xiaopei Lin[1], Zhaohui Chen[1] and Michael J. McPhaden[4]

The Paris Agreement aims to constrain global mean temperature (GMT) increases to 2 °C above pre-industrial levels, with an aspirational target of 1.5 °C. However, the pathway to these targets[1–6] and the impacts of a 1.5 °C and 2 °C warming on extreme El Niño and La Niña events—which severely influence weather patterns, agriculture, ecosystems, public health and economies[7–16]—is little known. Here, by analysing climate models participating in the Climate Model Intercomparison Project's Phase 5 (CMIP5; ref. 17) under a most likely emission scenario[1,2], we demonstrate that extreme El Niño frequency increases linearly with the GMT towards a doubling at 1.5 °C warming. This increasing frequency of extreme El Niño events continues for up to a century after GMT has stabilized, underpinned by an oceanic thermocline deepening that sustains faster warming in the eastern equatorial Pacific than the off-equatorial region. Ultimately, this implies a higher risk of extreme El Niño to future generations after GMT rise has halted. On the other hand, whereas previous research suggests extreme La Niña events may double in frequency under the 4.5 °C warming scenario[8], the results presented here indicate little to no change under 1.5 °C or 2 °C warming.

For a given rise in global mean temperature (GMT), regional climate impacts and local capacities to adapt vary vastly from one region to another. As such, there is debate as to what level of climate change is considered dangerous[18,19]. The local impacts projected for 2 °C warming are beyond what many societies can cope with[1,20,21]. A lower warming level has been called for and the historic Paris Agreement responded with an aspirational target of 1.5 °C. Limiting warming to 1.5 °C would reduce the projected frequency of heat extremes by 50% from that associated with 2 °C warming[22], and reduce the melting of polar ice sheets, which contributes directly to the risk of global sea level rise[23–25]. However, there are only a limited number of studies that have looked into the impacts associated with 1.5 °C warming, with most studies conducted in the context of 2 °C warming. Here we assess the impact of 1.5 °C warming on the frequency of extreme El Niño and extreme La Niña events, such as those that occurred respectively in 1997 and 1998, and caused global socio-economic and environmental disruptions[9–16].

During extreme El Niño events, atmospheric convection shifts into the otherwise cold and dry eastern equatorial Pacific (Niño3 region, 5° S–5° N, 150° W–90° W)[7,26] (see Methods). A collapse of the 'northern off-equatorial-minus-equatorial' sea surface temperature (SST) gradient allows the Intertropical Convergence Zone (ITCZ) to migrate southwards to the Niño3 region[7]. An extreme La Niña (see Methods) features concentrated warming and atmospheric convection in the Maritime region but cooling and reduced convection in the central equatorial Pacific[8,27]. The cooling is supported by stronger easterly winds driven by an enhanced Maritime-minus-central Pacific zonal temperature gradient, inducing upwelling of cool subsurface water in the central equatorial Pacific. Under a business-as-usual scenario, that is, Representative Concentration Pathway 8.5 (RCP8.5)[2], in which GMT increases by about 4.5 °C by 2100, greenhouse warming leads to an increased frequency of extreme El Niño and extreme La Niña events[7,8]. The eastern equatorial Pacific (central region of extreme El Niño anomalies) is projected to warm faster than the surrounding regions, causing the mean meridional SST gradient to decrease[7], and Niño3 rainfall to increase. Further, the Maritime region is projected to warm faster than the central equatorial Pacific (core to La Niña anomalies[27]), leading to an enhanced Maritime-minus-central Pacific zonal gradient[8]. Consequently, it is easier to induce extreme El Niño and extreme La Niña events[7,8].

However, as the global community aims to limit warming below 1.5 °C, it is critical to evaluate the risk of extreme El Niño and extreme La Niña in a 1.5 °C warming world. It is also of interest to compare this with the less ambitious target of 2 °C warming. Here we show that, although lower from the 2 °C warming level, the frequency of extreme El Niño at 1.5 °C warming doubles from that of the pre-industrial level, and continues to increase long after the GMT stabilizes.

In the Climate Model Intercomparison Project's Phase 5 (CMIP5; ref. 17), the RCP2.6 'peak and decline' emissions scenario, with CO_2 stabilizing at 450 ppm around 2040 and declining thereafter[2], is the only pathway available to limit a peak GMT rise close to 1.5 °C above the pre-industrial level. We use a total of 13 available models forced under this emissions scenario on the basis of their ability to generate extreme El Niño and La Niña events[7,8]. To determine the timing of 1.5 °C warming, we calculate 31-year running averages of the GMT in each model. The frequency of the extreme events over the 31-year period closest to this warming level is compared with that from a 31-year pre-industrial period (1869–1899), a period that is common across the 13 models. Varying the window length to 21, 41, or 51 years produces similar results (Supplementary Figs 1–4). We focus on the months of December, January and February, or boreal winter, in which an El Niño/La Niña event peaks. Because the warming in the majority of these experiments under RCP2.6 does not reach 2 °C, we adopted the approach[28] of using RCP2.6 for 1.5 °C warming and RCP4.5 for 2 °C warming to explore their differences. The RCP4.5 pathway is a scenario in which the total radiative forcing increases until 2100[2].

[1]Physical Oceanography Laboratory/CIMST, Ocean University of China and Qingdao National Laboratory for Marine Science and Technology, Yushan Road, Qingdao 266003, China. [2]Centre for Southern Hemisphere Oceans Research (CSHOR), CSIRO Oceans and Atmosphere, Hobart 7004, Australia. [3]Australian Research Council (ARC) Centre of Excellence for Climate System Science, Level 4 Mathews Building, The University of New South Wales, Sydney 2052, Australia. [4]NOAA/Pacific Marine Environmental Laboratory, Seattle, Washington 98115, USA. *e-mail: wenju.cai@csiro.au; lxwu@ouc.edu.cn

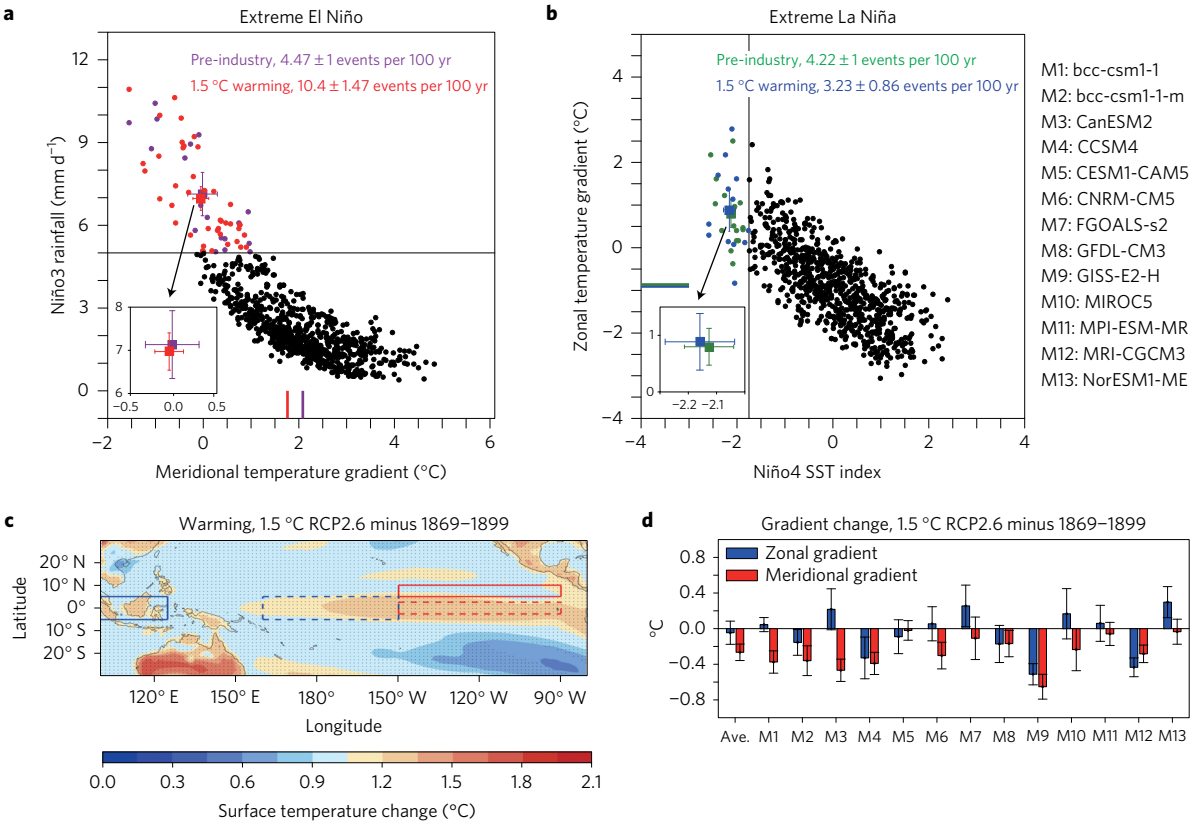

Figure 1 | Changes associated with 1.5 °C warming from the pre-industrial level. a, Boreal winter relationship between total rainfall (mm per day) in the Niño3 area and meridional surface temperature gradient (°C) (red solid area minus red dashed area in **c**) for pre-industrial and targeted 1.5 °C warming levels, with extreme El Niño events identified in purple and red, respectively. **b**, As for **a** but for Niño4 SST anomalies and zonal surface temperature gradient (°C) (blue solid minus blue dashed area) based on 13 models (listed), with extreme La Niña events identified in green and blue, respectively. The black dots in **a** and **b** indicate events that are not extreme. The corresponding multi-model means and their uncertainties based on a Student's *t*-test at the 90% confidence level are indicated by a square with error bars. The corresponding average frequency for the pre-industrial condition and the targeted warming levels is labelled in the top right corner of each panel, with the 90% confidence intervals based on a Poisson distribution. The frequency change in extreme El Niño events is in fact significant above the 99% confidence level (4.47 ± 1.55 for the pre-industrial, and 10.4 ± 2.31 for the 1.5 °C warming), without involving statistically significant change in the rainfall intensity (inset). The change in extreme La Niña frequency is not statistically significant. Short colour bars near an axis in **a** and **b** indicate climatological mean SST gradients for each period. **c**, Multi-model ensemble mean changes in surface temperature anomalies. Stippled areas indicate regions where the differences are significant above the 90% confidence level, determined by a two-sided Student's *t*-test. **d**, Changes in mean zonal (blue bars) and meridional (red bars) temperature gradient for multi-model ensemble (MME) average and each of the 13 models. The error bars correspond to the 90% confidence level (see Methods).

At 1.5 °C warming, the frequency of extreme El Niño (events with Niño3 rainfall exceeding a threshold of 5 mm d^{-1} within each 31-yr window; see Methods) increases from 18 events over 403 years, or about 4.5 events per 100 years (that is, one event per 22 years) in the pre-industrial period (Fig. 1a), to 42 events over 403 years, or 10.4 events per 100 years (that is, about one event per 10 years). This 130% increase is statistically significant above the 90% confidence level (Methods), and is in fact above the 99% confidence (see Fig. 1 caption). The inter-model consensus is strong, with none of the models producing a reduction. The result holds after the mean rainfall trend is removed (Methods). Although the frequency increases, the intensity of the extreme El Niño shows little change (shown in a square with error bars).

The emerging warming pattern features a faster warming in the eastern equatorial Pacific, in which the mean climatological meridional temperature gradient decreases as the eastern equatorial Pacific warms (Fig. 1c). This is underscored by a strong inter-model consensus (red bars in Fig. 1d). The changes on average are over four times greater than the magnitude of internally generated decadal variability (Supplementary Table 1). In the majority of models the reduction in the mean meridional temperature gradient is statistically significant above the 90% confidence level, and the multi-model ensemble average is significant above the 99% confidence level. These features are also seen at 2 °C warming, but the frequency of extreme El Niño events is about 24% higher (Supplementary Fig. 5a).

By contrast, there is no discernible change in the frequency of extreme La Niña events (Fig. 1b and Supplementary Fig. 5b). Because a large portion of the Maritime region is ocean, a substantial warming contrast between the Maritime region and the central Pacific is harder to establish under moderate greenhouse warming in RCP2.6 or RCP4.5. Even in the business-as-usual RCP8.5 scenario, a well-defined increase in the mean zonal temperature gradient and extreme La Niña frequency occurs after around 2040 (Supplementary Fig. 6). As such, there is no inter-model consensus in the change of the zonal temperature gradient (blue bars in Fig. 1d and Supplementary Fig. 5d), nor in extreme La Niña frequency (Fig. 1b and Supplementary Fig. 5b) in the less aggressive emission scenarios. Thus, a direct consequence of the 1.5 °C and 2 °C warming target is no statistically significant increase in extreme La Niña, in contrast to that projected under RCP8.5 (ref. 8).

During the transient increase of CO_2, the risk of extreme El Niño appears to increase linearly with the rise in GMT. This underpins the difference in extreme El Niño frequency between

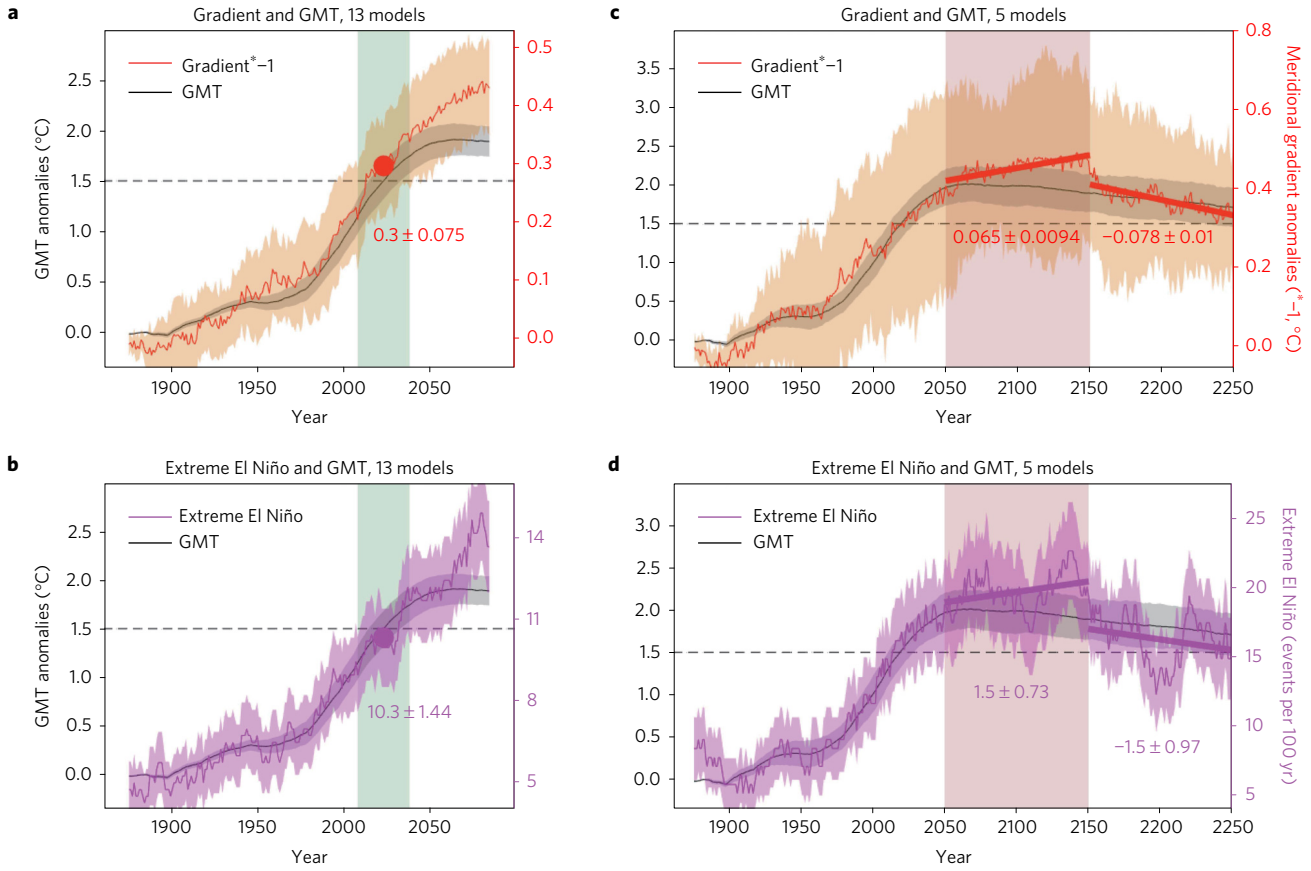

Figure 2 | Temporal evolution of multi-model ensemble mean changes under the RCP2.6 scenario. a, GMT anomalies (black curve) and meridional temperature gradient anomalies (sign-reversed, red curve) referenced to the pre-industrial condition (1869–1899) and averaged over 31-year sliding windows from 1869 to 2099. Their 90% confidence intervals are indicated by grey and light orange shades, respectively, based on a Student's *t*-distribution. The value near the red circle indicates the average over the 31 years centred at 1.5 °C warming (light green filled zone). **b**, The same as **a**, but for the frequency of extreme El Niño events (purple curve, events per 100 years). The 90% confidence intervals (light purple shades) are estimated based on a Poisson distribution (Methods). The value near the purple circle indicates the average over the 31 years centred at 1.5 °C warming (light green filled zone). Results are based on 13 available models. **c**,**d**, The same as **a** and **b**, respectively, but using five models with extended simulations to the 23rd century. The linear trends and their 90% confidence intervals over the 2050–2150 period and the 2151–2250 period indicate that although the GMT decreases, the meridional temperature gradient continues to weaken and the extreme El Niño frequency continues to increase before they reverse.

1.5 °C and 2 °C warming as reported above. To assess whether this linearity is systematic and robust, we examine the evolution of the GMT change, the meridional temperature gradient change, and the frequency of the extreme El Niño using 31-year sliding periods in each of the 13 models forced under historical emissions and the RCP2.6 scenario, and in terms of multi-model ensemble average (Fig. 2a,b, note the reversed gradient sign). The evolution shows that during the transient increase of CO_2 under RCP2.6, that is, prior to around 2050, the weakening meridional gradient and the increasing frequency change approximately linearly with the GMT rise. This is also seen in RCP4.5 (Supplementary Fig. 7). The linearity delivers a simple but powerful message that any increase in CO_2 matters in terms of extreme El Niño risk.

However, the ultimate risk is greater than that seen at 1.5 °C warming, as the frequency of extreme El Niño events continues to increase after the GMT peaks and stabilizes beyond 2050, from about 10 events per 100 years (multi-model ensemble average, purple filled circle in Fig. 2b) at 1.5 °C warming (light green filled zone) to about 14 events per 100 years beyond 2050. This is supported by a continued weakening in the mean meridional temperature gradient (Fig. 2a). The timescale for which further weakening may last, and the eventual frequency to which the further weakening may lead, are of great interest. There are only five models out of the 13 that have outputs beyond 2100, but we use these to provide a gauge (noting that an ensemble of five models will contain significant interdecadal variability). The weakening meridional gradient, established during the transient increase of CO_2, not only persists but actually intensifies for about a century (2050–2150) before reversing its trend to be in line with the GMT (Fig. 2c).

The frequency of extreme El Niño events, although defined using a discrete threshold value of rainfall and hence more fluctuating, essentially follows the same evolution, featuring a further increase after the GMT stabilizes (2050–2150, Fig. 2d). This is supported by a recent conclusion that an elevated risk of major disruption to rainfall over the Pacific appears locked in for at least the remainder of the twenty-first century[29], even if global warming is restricted to 2 °C. This behaviour is fairly similar to the response of sea level[23,24], but what is surprising is that even the temperature gradient, which measures the difference between two locations, responds in this manner.

The weakening of the mean meridional gradient is expected to relax as greenhouse gas emission levels off, but this does not happen until after about 2150 (see also Supplementary Fig. 8). The continued weakening is associated with stronger thermocline–SST coupling in the equatorial than the off-equatorial eastern Pacific. During the transient increase of CO_2 (prior to 2050) equatorial easterly winds weaken. Although the weakening easterly winds

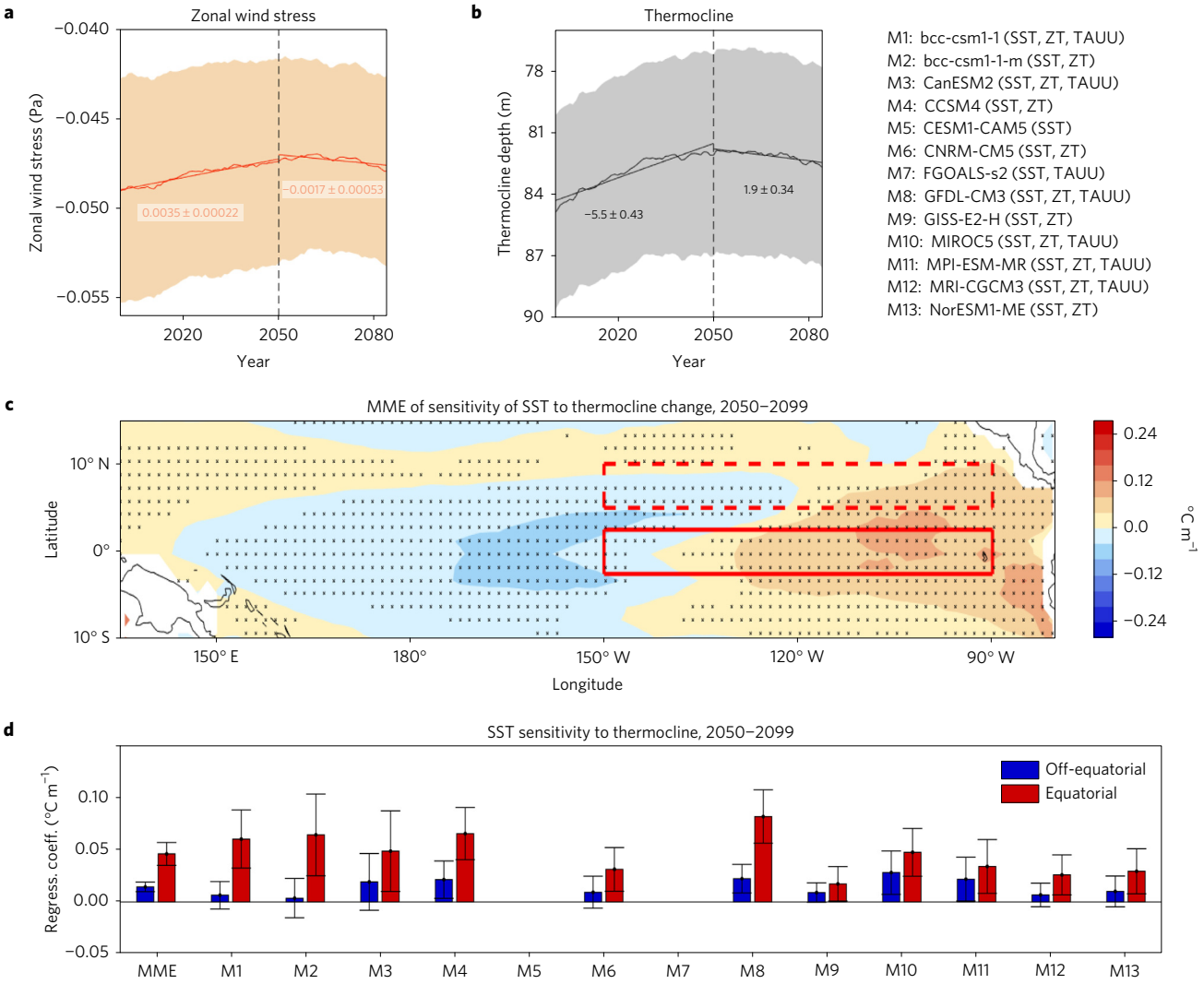

Figure 3 | Mechanism for a continuous increase in extreme El Niño frequency after emissions stabilize. a, Temporal evolution of 31-year sliding averages of zonal wind stress (Pa) over the eastern Pacific (10° S–10° N, 150° W–90° W) for seven models with available wind stress outputs (indicated by TAUU in the list of models, top right). The multi-model ensemble mean (red curve) and the 90% confidence intervals based on a Student's *t*-distribution (light orange) are indicated. A linear trend (Pa per 100 years) and its 90% confidence interval are provided for the 2000–2049 period and the 2050–2099 period. **b**, Same as **a**, but for thermocline depth (m) averaged over the same region, using 11 models with available data (indicated by ZT in the models list). In **b**, values on *y*-axis decrease upward. **c**, Multi-model ensemble mean of SST sensitivity to thermocline variability over the 2050–2099 period, calculated as regression coefficients between SST and thermocline depth at each grid point. Stippled areas indicate statistical significance above the 90% confidence level based on a Student's *t*-test. **d**, SST sensitivity to thermocline for each model for the off-equatorial (blue bars, dashed red area in **c**) and equatorial (red bars, solid red area in **c**) region. The 90% confidence intervals based on a Student's *t*-distribution are shown.

(or trend of anomalous westerly winds) lead to an ultimate shallowing of the thermocline, which alone would be conducive to a cooling through the thermocline coupling, the radiative forcing associated with increasing CO_2 dominates[30].

Once CO_2 stabilizes over the post-2050 period, several processes ensue: the radiative forcing diminishes, the equatorial easterly winds strengthen (Fig. 3a), and the thermocline deepens (Fig. 3b, note the reversed *y*-axis). The thermocline–SST coupling, whereby a deepening thermocline induces a surface warming, is far stronger in the eastern equatorial Pacific than off-equator. This is seen in the multi-model average (Fig. 3c) and in all individual models (Fig. 3d). This allows a more effective warming at the equator than off-equator by the deepening thermocline which offsets the diminishing radiative forcing. Thus, the faster warming at the equator than off-equator is continued, further reducing the meridional gradient and thus allowing a further increase in extreme El Niño frequency. This conclusion is supported by the close match between the persistent weakening of the meridional temperature gradient of −0.065 °C per 100 years after the GMT stabilization (Fig. 2c) and the product of the corresponding multi-model ensemble average thermocline deepening (1.9 m per 100 years; Fig. 3b) and the difference in the off-equatorial and equatorial SST–thermocline coupling (−0.033 °C m^{-1}; first two bars in Fig. 3d), which amounts to −0.063 °C per 100 years. The central point is that the ultimate risk can be substantially under-estimated when assessed using outputs from the transient increase of CO_2.

In summary, we have shown that the frequency of extreme El Niño events at 1.5 °C warming doubles that of the pre-industrial level, and continues to increase long after stabilization of the 1.5 °C warming. During the transient increase of CO_2, the frequency of extreme El Niño events evolves linearly with the rising GMT, conveying a simple but powerful message that any increase in CO_2 directly leads to a higher risk of an increased frequency of extreme El Niño events. This linear relationship attributed to

greenhouse forcing emerges because various other factors that influence the frequency of extreme El Niño in each model, such as decadal variability and weather noise, tend to be averaged out across an ensemble of models. The effects of these factors other than greenhouse forcing would be notable in a single realization, as in observation. Thus, future frequency increase due to greenhouse forcing in a single observed realization will continue to be influenced by internal variability and stochastic forcing. However, as we have shown here, the ultimate risk involves a continued increase in extreme El Niño frequency long after the GMT stabilization. This suggests a higher risk of extreme El Niño to future generations, and highlights the need to take into account the greater risks beyond the transient period.

Methods

Methods, including statements of data availability and any associated accession codes and references, are available in the online version of this paper.

Received 13 December 2016; accepted 22 June 2017; published online 24 July 2017

References

1. Meinshausen, M. *et al*. Greenhouse-gas emission targets for limiting global warming to 2 °C. *Nature* **458,** 1158–1162 (2009).
2. Moss, R. *et al*. The next generation of scenarios for climate change research and assessment. *Nature* **463,** 747–756 (2010).
3. Ranger, N. *et al*. Is it possible to limit global warming to no more than 1.5 °C? *Climatic Change* **111,** 973–981 (2012).
4. Luderer, G. *et al*. Economic mitigation challenges: how further delay closes the door for achieving climate targets. *Environ. Res. Lett.* **8,** 034033 (2013).
5. Rogelj, J., McCollum, D. L., O'Neill, B. C. & Riahi, K. 2020 emissions levels required to limit warming to below 2 °C. *Nat. Clim. Change* **3,** 405–412 (2013).
6. Rogelj, J. *et al*. Energy system transformations for limiting end-of-century warming to below 1.5 °C. *Nat. Clim. Change* **5,** 519–527 (2015).
7. Cai, W. *et al*. Increasing frequency of extreme El Niño events due to greenhouse warming. *Nat. Clim. Change* **4,** 111–116 (2014).
8. Cai, W. *et al*. More frequent extreme La Niña events under greenhouse warming. *Nat. Clim. Change* **5,** 132–137 (2015).
9. Philander, S. G. H. Anomalous El Niño of 1982–83. *Nature* **305,** 16 (1983).
10. Merlen, G. The 1982–1983 El Niño: some of its consequences for Galapagos wildlife. *Oryx* **18,** 210–214 (1984).
11. Glynn, P. W. & de Weerdt, W. H. Elimination of two reef-building hydrocorals following the 1982–83 El Niño. *Science* **253,** 69–71 (1991).
12. Vos, R., Velasco, M. & Edgar de Labastida, R. *Economic and Social Effects of El Niño in Ecuador, 1997–1998* Technical papers series POV-107, 38 (Inter-American Development Bank Sustainable Development Dept., 1999).
13. Aronson, R. B. *et al*. Coral bleach-out in Belize. *Nature* **405,** 36 (2000).
14. Bell, G. D. *et al*. Climate Assessment for 1998. *Bull. Am. Meteorol. Soc.* **80,** 1040 (1999).
15. McPhaden, M. J., Zebiak, S. E. & Glantz, M. H. ENSO as an integrating concept in Earth science. *Science* **314,** 1740–1745 (2006).
16. Vincent, E. M. *et al*. Interannual variability of the South Pacific Convergence Zone and implications for tropical cyclone genesis. *Clim. Dynam.* **36,** 1881–1896 (2011).
17. Taylor, K. E., Stouffer, R. J. & Meehl, G. A. An overview of CMIP5 and the experimental design. *Bull. Am. Meteorol. Soc.* **93,** 485–498 (2012).
18. Schellnhuber, H. J., Cramer, W., Nakicenovic, N., Wigley, T. M. L. & Yohe, G. (eds) *Avoiding Dangerous Climate Change* (Cambridge Univ. Press, 2006).
19. Mahlstein, I., Knutti, R., Solomon, S. & Portmann, R. W. Early onset of significant local warming in low latitude countries. *Environ. Res. Lett.* **6,** 034009 (2011).
20. *Submissions from Parties FCCC/KP/AWG/2009/MISC.1/Add.1* (UNFCCC, 2009).
21. *Climate Change 2014: Impacts, Adaptation, and Vulnerability* (eds Field, C. B. *et al*.) 1–32 (IPCC, Cambridge Univ. Press, 2014).
22. Fischer, E. M. & Knutti, R. Anthropogenic contribution to global occurrence of heavy-precipitation and high-temperature extremes. *Nat. Clim. Change* **5,** 560–564 (2015).
23. Schaeffer, M., Hare, W., Rahmstorf, S. & Vermeer, M. Long-term sea-level rise implied by 1.5 °C and 2 °C warming levels. *Nat. Clim. Change* **2,** 867–870 (2012).
24. Levermann, A. *et al*. The multimillennial sea level commitment of global warming. *Proc. Natl Acad. Sci. USA* **110,** 13745–13750 (2013).
25. Dutton, A. *et al*. Sea level rise due to polar ice-sheet mass loss during past warm periods. *Science* **349,** aaa4019 (2015).
26. Lengaigne, M. & Vecchi, G. A. Contrasting the termination of moderate and extreme El Niño events in coupled general circulation models. *Clim. Dynam.* **35,** 299–313 (2009).
27. Takahashi, K., Montecinos, A., Goubanova, K. & Dewitte, B. ENSO regimes: reinterpreting the canonical and Modoki El Niño. *Geophys. Res. Lett.* **38,** L10704 (2011).
28. Knutti, R., Rogelj, J., Sedlacek, J. & Fischer, E. M. A scientific critique of the two-degree climate change target. *Nat. Geosci.* **9,** 13–18 (2016).
29. Power, S. P. *et al*. Humans have already increased the risk of major disruptions to Pacific rainfall. *Nat. Commun.* **8,** 14368 (2017).
30. Liu, Z., Vavrus, S., He, F., Wen, N. & Zhong, Y. Rethinking tropical ocean response to global warming: the enhanced equatorial warming. *J. Clim.* **18,** 4684–4700 (2005).

Acknowledgements

This work is supported by Centre for Southern Hemisphere Oceans Research. W.C. and G.W. are supported by the Earth Science and Climate Change Hub of the Australian Government's National Environmental Science Programme, and a CSIRO Office of Chief Executive Science Leader award. A.S. is supported by the Earth Science and Climate Change Hub of the Australian Government's National Environmental Science Programme and the Australian Research Council. PMEL contribution 4427.

Author contributions

W.C. and G.W. conceived the study. G.W. performed all model analysis. W.C. wrote the initial manuscript with support from A.S. and G.W. All authors contributed to interpreting results, discussion of the associated dynamics, and improvement of this paper.

Additional information

Supplementary information is available in the online version of the paper. Reprints and permissions information is available online at www.nature.com/reprints. Publisher's note: Springer Nature remains neutral with regard to jurisdictional claims in published maps and institutional affiliations. Correspondence and requests for materials should be addressed to W.C. or L.W.

Competing financial interests

The authors declare no competing financial interests.

Methods

Definition of extreme El Niño. Extreme El Niño events are characterized by an exceptional warming extending into the eastern equatorial Pacific[9,15]. The high sea surface temperatures (SST) lead to an equatorward shift of the Intertropical Convergence Zone (ITCZ), and hence intense rainfall in the equatorial eastern Pacific (Niño3 area: 5° S–5° N, 150° W–90° W) where cold and dry conditions normally prevail. Niño3 rainfall is thus a good indicator of extreme El Niño[7,26]. An extreme El Niño is defined as an event during which such massive reorganization of atmospheric convection takes place, leading to Niño3 rainfall that exceeds 5 mm per day averaged over the El Niño mature season of December, January and February[7]. This definition distinctly identifies the 1982/83 and 1997/98 events as extreme El Niño.

Extreme El Niño and mean rainfall trend. Given that mean Niño3 rainfall increases under greenhouse warming, a question arises as to how the mean rainfall increase affects the frequency change. The mean rainfall trend includes changes contributed by the mean-state change, and changes due to the increased frequency of extreme El Niño frequency.

To determine the first contribution, we exclude samples in which Niño3 rainfall is greater than 5 mm d^{-1} (our original definition of extreme El Niño events) in all models. A new multi-model ensemble average time series and its linear trend are then constructed. The trend is 0.21 mm per day per 100 years, and this is taken as the mean-state change without the contribution from extreme El Niño. This is nearly 45% smaller than the total trend of 0.38 mm per day per 100 years, suggesting that aggregated over all 13 models the increased frequency contributes nearly 45% to the mean Niño3 rainfall increase. Therefore, we remove the trend due to mean-state change only by applying the same procedure to an individual model (that is, in each model, calculate and remove the individual model trend without the contribution from extreme El Niño). The frequency increases from 3.97 (instead of the original 4.47) to 8.68 (instead of the original 10.4) events per 100 years; that is, a 118% increase. This compares well with the 130% increase in the original result. Using a quadratic detrending yields almost the same result. We conclude that the mean rainfall increase does not change our results in any material way.

Eastern equatorial Pacific meridional SST gradients. During extreme El Niño events, warming in the eastern equatorial Pacific dramatically weakens the meridional SST gradient. This gradient measures the difference between the northern off-equatorial (5°–10° N, 150°–90° W, that is, the present-day climatological ITCZ position) and the equatorial Pacific (2.5° S–2.5° N, 150°–90° W) (red solid box minus red dashed box, Fig. 1c). Convection follows the highest SSTs; as such, the ITCZ shifts equatorward[7,26] leading to atmospheric convection and extraordinary rainfall (>5 mm per day) in the normally dry eastern equatorial Pacific. The smaller the gradient, the greater ease for this to occur.

Definition of extreme La Niña. An extreme La Niña is not the opposite of an extreme El Niño[27]. During extreme La Niña events, coldest sea surface conditions develop in the central Pacific[27] inhibiting formation of rain-producing clouds there, but enhancing atmospheric convection and rainfall in the western equatorial Pacific. An extreme La Niña event is defined as one for which the amplitude of central equatorial Pacific (Niño4, 5° S–5° N, 160° E–150° W) SST anomalies, referenced to the pre-industrial climatology and then quadratically detrended, is greater than a 1.75 pre-industrial standard deviation (s.d.) value in the La Niña mature season, that is, December, January and February.

Maritime-minus-central Pacific SST gradient. During extreme La Niña events, coldest sea surface conditions develop in the central Pacific, creating an enhanced temperature gradient from the Maritime continent to the central Pacific. This cooling generates stronger easterly winds, which pile up warm water in the western Pacific, increasing the Maritime–central Pacific temperature gradient[8] (defined as the average over 5° S–5° N, 100° E–125° E minus the average over 5° S–5° N, 160° E–150° W) (blue solid box minus blue dashed box, Fig. 1c). This in turn generates further anomalous upwelling of cool water to the surface, and westward surface currents in the Niño4 region, conducive to growth of cold anomalies in the region, in a positive feedback. An increasing trend of this gradient is conducive to occurrences of this positive feedback.

Model selection. We used CMIP5 model outputs of surface temperature, precipitation, zonal surface wind stress and ocean temperature to calculate thermocline depth, under the RCP2.6 'peak and decline' emissions scenario, for the boreal winter season (December, January and February), in which an El Niño event matures. In RCP2.6, CO_2 stabilizes at 450 ppm around 2040 and declines thereafter[2]. This is the only pathway available to limit a peak GMT rise close to 1.5 °C above the pre-industrial level. A total of 13 models are used, which were selected by a previous study[7] for their ability to simulate extreme El Niño events leading to a positive skewness in eastern equatorial Pacific rainfall. Models that are unable to simulate such events in the first place clearly cannot be used to make future projections of such events. Furthermore, all the selected models must be able to reach a 1.5 °C warming under the RCP2.6 scenario. We took a 31-year period centred at the warming of 1.5 °C under the RCP2.6 scenario, and 2 °C under RCP4.5, relative to the pre-industrial period of 1869–1899. The choice of the length is a balance between two factors. If the period span is too short, the number of extreme El Niño events within each window would tend to be too small (because the frequency is about one event in 10 to 20 years); on the other hand, if the period is too long, it will capture warming that is both far smaller and far greater than the targeted 1.5 °C, as well as shortening the time series for examining the time-varying response (for example, Fig. 2). Either case would make it less effective in assessing the link between the frequency and background warming. Changing the window length to 21, 41, or 51 years does not modify our results (Supplementary Figs 1–4). Note that these simulations are transient and an equilibrium state does not exist for most models. The first ensemble member from each model is used with equal weight across models. To compare the changes at 1.5 °C warming with the internally generated interdecadal variability, we have also used data from the pre-industrial control experiment (Supplementary Table 1).

Statistical significance tests. We applied various statistical tests to assess the significance of our results based on multi-model aggregation. In terms of frequency of extreme El Niño and extreme La Niña events, we chose a Poisson distribution, which is suitable for a discrete probability distribution that expresses the probability of a given number of events occurring in a fixed interval of time. The Poisson confidence intervals are estimated, using the MATLAB software package, which calculates a given confidence interval for Poisson data (that is, frequency of extreme El Niño events in Figs 1a,b and 2b,d, and places throughout the text). Otherwise, we use a Student's *t*-test. Unless otherwise stated, statistical significance is based on a 90% confidence interval, and the number of degrees of freedom is simply the number of models, as each model is regarded as an independent sample.

To estimate the uncertainties associated with the change in the zonal gradient and meridional gradient between a 1.5 °C warming world and the pre-industrial period (Fig. 1d and Supplementary Fig. 5d), which is expressed as a difference between two 31-year periods, for each model we first quadratically detrend the entire time series of the gradient (1869–2100), and apply a 31-year sliding window to calculate the running average of the gradient. We then randomly select two values 10,000 times and calculate their difference to obtain 10,000 realizations of such differences. The 90% confidence interval based on these 10,000 realizations is then estimated. A statistically significant result means the difference between the 1.5 °C warming world and pre-industrial period in each model is significant beyond the approximate range of natural variability in that model. For the multi-model ensemble difference, the confidence interval is based on the inter-model spread using a Student's *t*-distribution.

Changes in extreme La Niña frequency. There is no inter-model consensus on the change in extreme La Niña frequency between the pre-industrial and the 1.5 °C warming world. The ensemble differences are not statistically significant at the 90% confidence level: 3.23 ± 0.86 events per 100 years at 1.5 °C warming (the errors correspond to the 90% confidence interval determined from a Poisson distribution), and 4.96 ± 1.06 events per 100 years at 2.0 °C warming from the pre-industrial level (4.22 ± 1.0 events per 100 years). The frequency of the catastrophic combination of an extreme El Niño event followed by an extreme La Niña event, as seen in 1997 and 1998, shows no significant difference between the pre-industrial (0.98 ± 0.50 events per 100 years) and 1.5 °C warming (0.99 ± 0.50 events per 100 years). However, the frequency of this sequence increases to 2.73 ± 0.79 events per 100 years at 2 °C warming, significantly greater than that at 1.5 °C warming. This suggests that reducing warming from 2 °C to 1.5 °C presents the potential to reduce the 1997–98 type of catastrophic swing in extremes.

Data availability. All data supporting the findings of this study are available from the corresponding authors upon request.